The flood case 27–29 July 2004

SAMI NIEMELÄ
Finnish Meteorological Institute, P.O.Box 503, FI-00101 Helsinki, Finland

1 Introduction

The southern and central parts of Finland received very large precipitation amounts during 27–29 July 2004 due to a slowly moving low pressure system. This rain event caused flooding over large areas. Fig. 1a shows radar retrieved 12-hour accumulated precipitation amount valid at 12 UTC 29 July 2004. This illustrates that the low pressure system remained nearly stationary over Gulf of Finland. Consequently, the main precipitation area was located over Southern Finland and western part of the Gulf. At that time, the maximum precipitation amounts obtained were between 40–50 mm $12h^{-1}$. The reference HIRLAM, ran operationally at FMI with a horizontal resolution of 22 km (RCR starting from 12 UTC 27 July 2004), failed to produce such strong precipitation amounts as were observed during this two day period.

The objective of this study is to clarify the following questions. Can we make better precipitation forecasts just by reducing the grid size? Can we even simulate the structure of the precipitation event with meso-γ-scale HIRLAM? In this study, we also compare the nonhydrostatic version of HIRLAM (Rõõm, 2001) with the traditional hydrostatic HIRLAM. The different meso-γ-scale model configurations are validated using data from FMI's radar network. Modelled radar reflectivites, which are computed by using the Radar Simulation Model (Haase and Fortelius, 2001), produced by non-operational experiments can be compared directly with observations. More detailed description of the study is presented by Niemelä and Loridan (2004)

2 Experimental setup

Several experiments, both simulations and forecasts, are conducted in order to study the extreme precipitation event. FMI's operational forecasts (RCR and MBE with 22 and 9 km grid size, respectively) and one ECMWF forecast are also used in the evaluation. The analysis time of the operational HIRLAM forecasts is 12 UTC 27 July 2004, whereas ECMWF forecast started at 06 UTC 27 July 2004 (RCR's boundary field). Experimental forecasts with 5.6 km grid size, both hydrostatic (HH) and nonhydrostatic (NH), are made in order to study the effect of resolution on the precipitation forecast. The main differences to operational suites are the nonhydrostatic dynamics of NH and partly modified physical parameterizations in both HH and NH. The modifications in physics mainly involve changes in convection and condensation scheme (Straco, Sass, 2002) and turbulence scheme (CBR). These changes should be considered as "tuning", which aims to make these schemes more applicable in higher resolution (Δx $\leq$10 km). The meso-γ-scale HIRLAM simulations (HH and NH with MBE analyses as boundaries), utilizing both 5.6 and 2.8 km grid size, try to find an answer to the second question, which was mentioned at the end of Section 1.

3 Results

3.1 Forecasts

Fig. 1 shows 12-hour precipitation amount [mm] accumulated during 36–48 hour forecast period (in ECMWF case 42–54 h). ECMWF model (panel b) is able to predict the location of the low pressure center fairly well. Concequently, the loaction of the main precipitation area is also well predicted. However, ECMWF seems to produce too much precipitation over the central parts of Finland.

Both operational HIRLAM forecasts, panels c and d, clearly misplace the low pressure center about 300 km to south-west from the observed location. Consequently, the areas with heaviest predicted precipitation are also located in wrong place. RCR underestimates the maximum precipitation by about 20–25 mm, whereas MBE creates maximum rainfall more close to observed one.

Both experimental forecasts (5.6 km grid size) also misplace the low pressure center (panels e and f). This is a clear example of how the forecasts, with small integration domain, are "slaves" of their lateral boundaries. NH produces similar precipitation distribution as MBE, whereas HH seems to overestimate the precipitation amount. The maximum precipitation amount produced by HH is clearly too strong.

Fig. 2 shows the time series of areal averaged 12-hour accumulated precipitation amount. On the average, coarser resolution ECMWF and RCR produce less precipitation than MBE, HH and NH. In this case, the precipitation amount produced by the higher resolution models are closer to radar observations (not shown). HH and NH behaves similarly than MBE and therefore do not bring any extra value to the average precipitation. However, HH and NH generate locally more intense precipitation rates compared to MBE, as shown in Fig. 1.

3.2 Simulations

Fig. 3 shows the instantaneous radar reflectivity fields from the model experiments (panels a–d) and the corresponding observations (panels e–f) valid at 12 UTC 29 July. Both hydrostatic experiments (a - 5.6 km and b - 2.8 km) create wide precipitation cells with strong reflectivity (>40 dBZ), which are not observed. However, nonhydrostatic results are more congruent with observations.

Fig. 4 presents frequency distributions of radar reflectivity from both model experiments and observations. All the distributions are gathered during the 54 hour simulations. Nonhydrostatic experiments with 5.6 and 2.8 km grid length represent the distribution of moderate and strong reflectivites (>24 dBZ) very well, whereas hydrostatic models clearly overestimate. The overestimation by HH is much more prominent with the 2.8 km grid size. The difference between NH experiments with different resolutions is smaller. It seems that the higher resolution NH slightly underestimates the amount of strong reflectivities (>32 dBZ) in general. However, both HH and NH, with the 2.8 km grid size, produce reflectivities over 48 dBZ ($\approx$ 24 mm h^{-1})

in some grid cells. HH does it even with the 5.6 km grid size. Consequently, models produce locally too much precipitation (100–150 mm $12h^{-1}$, not shown). Such high values are about 2–3 times more than observed rainfall.

The amount of reflectivities below 24 dBZ is clearly overestimated by all experiments. This basically means that the model creates wider precipitation areas with weak intensity compared to obserevations. One reason to overestimation can be seen from Figs. 3d and 3f. Models cannot resolve highly scattered, smallest scale convective precipitation cells (in panel f). Instead, they produce smoother precipitation fields with weak intensity (panel d).

4 Conclusions

During 27–29 July 2004 extreme precipitation event swept over southern and central Finland creating flooding over large areas. Operational forecast of FMI starting from 12 UTC 27 July 2004 failed to produce high precipitation amounts at right locations. Therefore, several model forecasts and simulations of this event has been conducted in order to study the possible additional value of meso-γ-scale HIRLAM.

- Obviously, the location of the precipitation can not be improved just by reducing the grid size. If the outer model fails to produce the prevailing synoptic conditions, surely the inner model can not do any better. This just emphasize the important role of the high-quality synoptic-scale model as part of the meso-γ-scale NWP system.
- However, the average precipitation amount can be increased, and in this case improved, by reducing the grid size from 22 to 9 km. By reducing the grid size from 9 km further to 5.6 km does not have such a big impact on the average (locally the impact is larger).
- Nonhydrostatic model combined with the Straco-scheme and the 5.6 km grid, can produce realistic reflectivity distribution. However, models utilizing the 2.8 km grid size tend to produce too much precipitation. Hydrostatic model overestimates the amount of strong reflectivities with both resolutions.

References

Haase, G. and C. Fortelius, 2001: Simulation of radar reflectivities using Hirlam forecasts. HIRLAM Tech. Rep. 51, SMHI, S-601 76 Norrköping, Sweden. Hirlam-5 Project, 22 pp.

Niemelä, S. and T. Loridan, 2004: The flood case 27–29 July 2004: added value of the meso-γ-scale HIRLAM? *HIRLAM newsletter*, **46**, 48–58.

Rõõm, R., 2001: Nonhydrostatic adiabatic kernel for HIRLAM. Part I: Fundamentals of nonhydrostatic dynamics in pressure-related coordinates. HIRLAM Tech. Rep. 48, SMHI, S-601 76 Norrköping, Sweden. Hirlam-5 Project, 25 pp.

Sass, B. H., 2002: A research version of the STRACO cloud scheme. DMI Tech. Rep. 02-10, Danish Meteorological Institute, DK-2001 Copenhagen, Denmark. 25 pp.

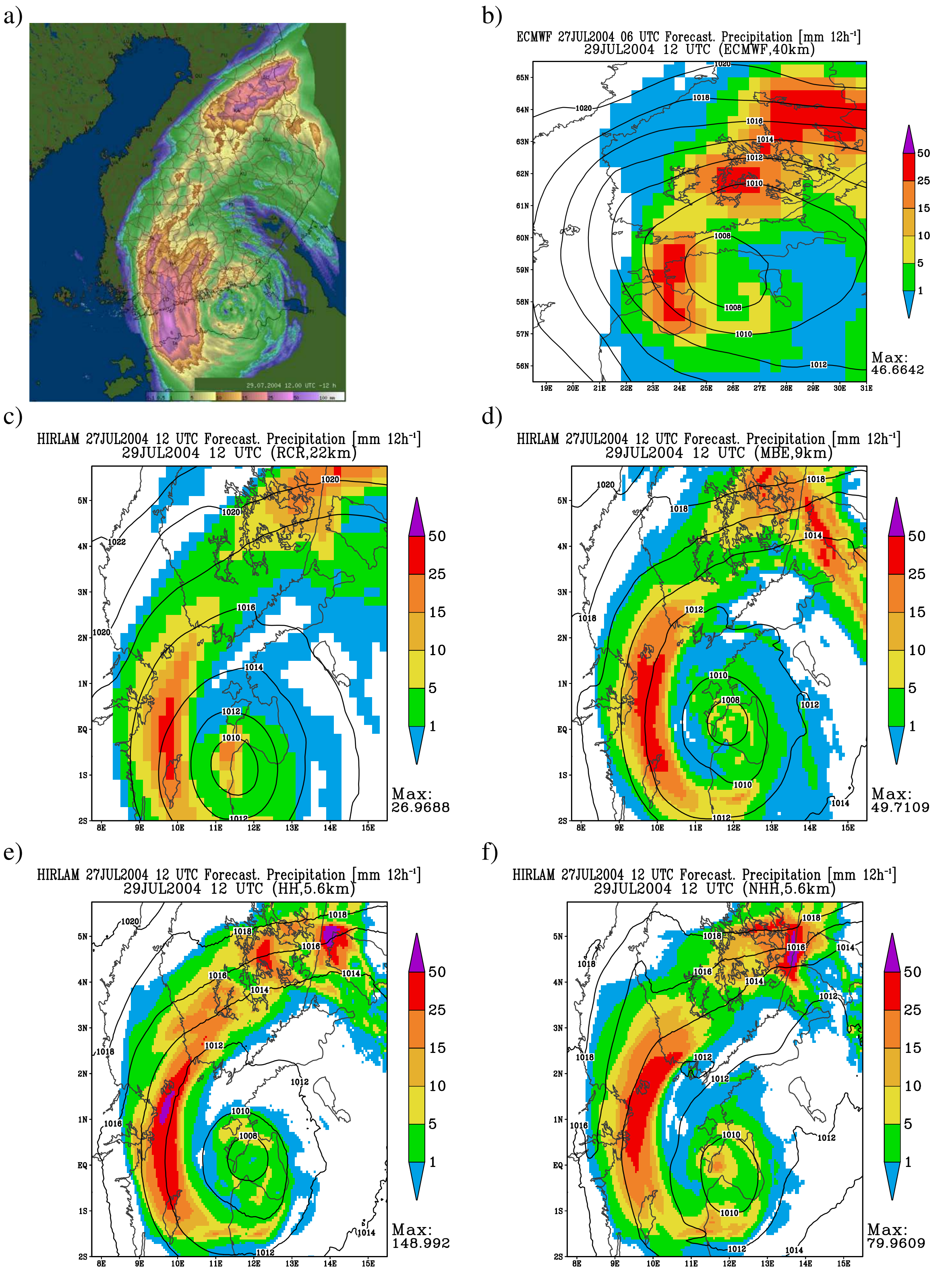

Figure 1: 12-hour accumulated precipitation [mm] and mean sea level pressure [hPa] valid at 12 UTC 29 July 2004. a) Observation retreived from the FMI's radar network and the forecasts from b) ECMWF 40 km, c) RCR 22 km, d) MBE 9 km, e) HH 5.6 km and f) NH 5.6 km.

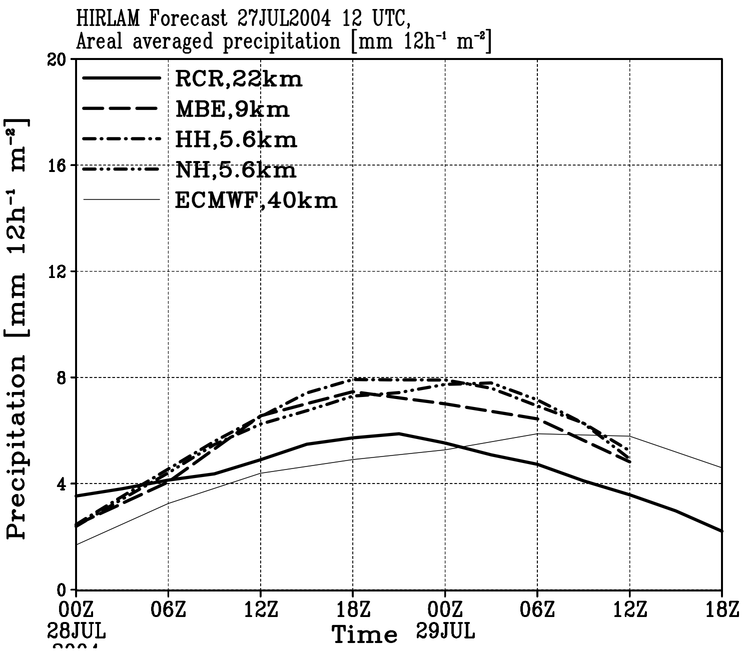

Figure 2: Time series of the areal averaged 12-hour accumulated precipitation [mm]. Forecasts averaged over the area seen in Fig. 1c: solid (thick) = RCR, 22 km, dashed = MBE, 9 km, dot-dashed = HH, 5.6 km, dot-dot-dashed = NH, 5.6 km and solid (thin) = ECMWF, 40 km.

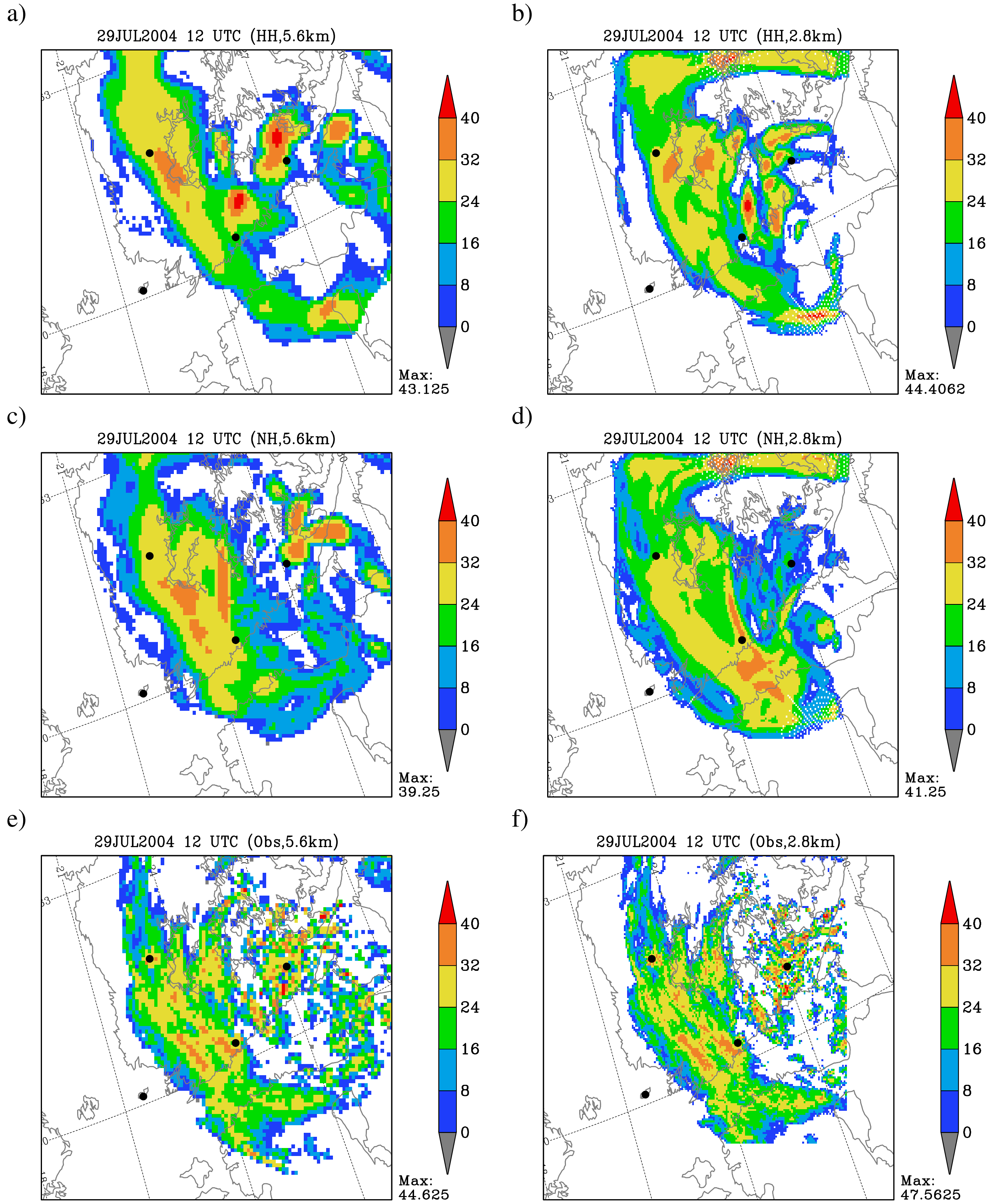

Figure 3: Composite of radar reflectivity [dBZ] fields after 48 hour simulation valid at 12 UTC 29 July 2004. a) HH, 5.6 km, b) HH, 2.8 km, c) NH, 5.6 km, d) NH, 2.8 km, e) radar observation, 5.6 km and f) radar observation, 2.8 km. The locations of the radars are marked with black dots.

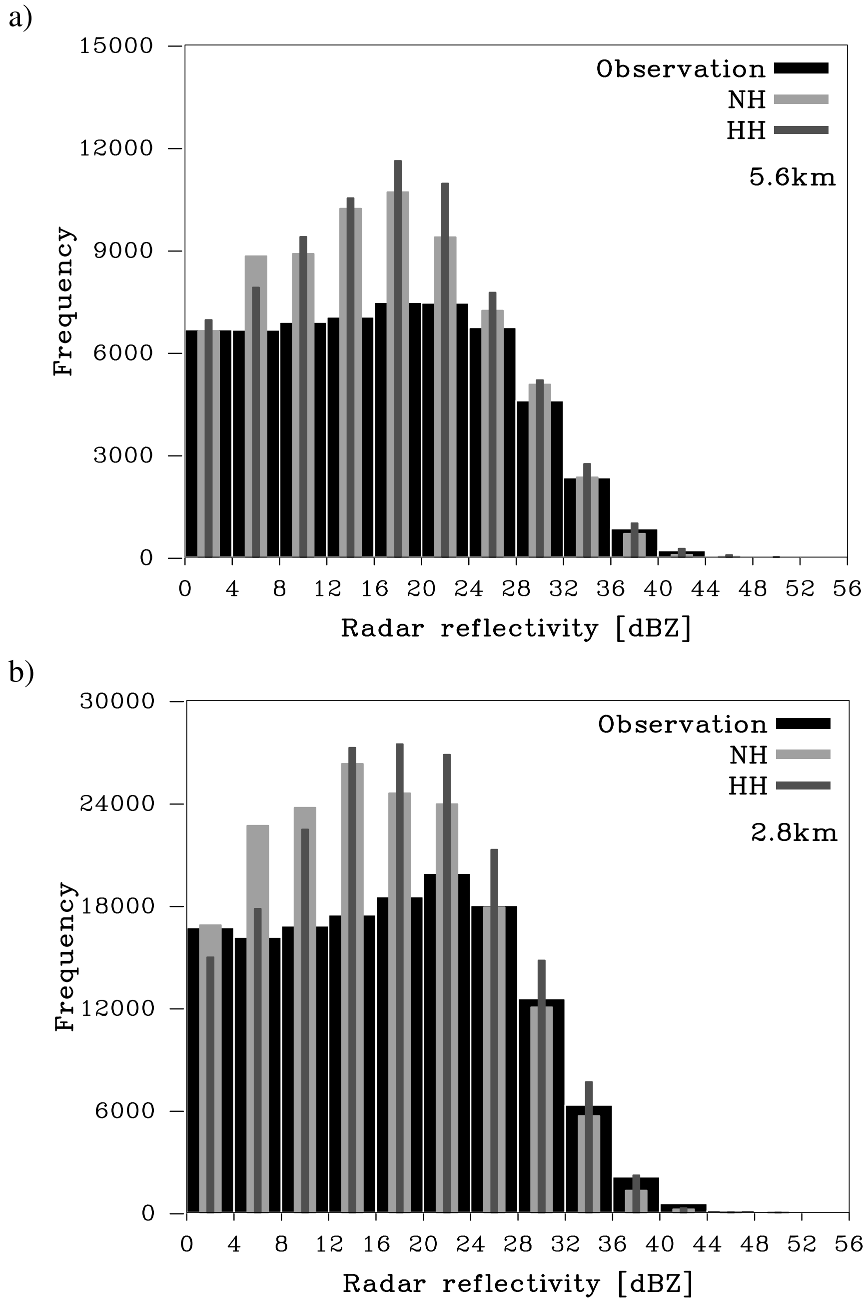

Figure 4: Frequency distributions of radar reflectivity [dBZ] produced by 54 hour simulations starting from 12 UTC 27 July 2004. Grid length is a) 5.6 km and b) 2.8 km. NH- and HH-experiments are represented with light gray and dark gray bars, respectively. Black bars represent dBZ-observations. The elevation of radar antenna is 0.4°. In this case reflectivity values below 0 dBZ are not meteorologically important and therefore those are omited.